Environmental Science & Technology

pubs.acs.org/est

Article

Pseudomonas sp. Strain 273 Incorporates Organofluorine into the Lipid Bilayer during Growth with Fluorinated Alkanes

Yongchao Xie, Amanda L. May, Gao Chen, Lindsay P. Brown, Joshua B. Powers, Eric D. Tague, Shawn R. Campagna,* and Frank E. Löffler*

Cite This: *Environ. Sci. Technol.* 2022, 56, 8155−8166

Read Online

ACCESS | Metrics & More | Article Recommendations | Supporting Information

ABSTRACT: Anthropogenic organofluorine compounds are recalcitrant, globally distributed, and a human health concern. Although rare, natural processes synthesize fluorinated compounds, and some bacteria have evolved mechanisms to metabolize organofluorine compounds. *Pseudomonas* sp. strain 273 grows with 1-fluorodecane (FD) and 1,10-difluorodecane (DFD) as carbon sources, but inorganic fluoride release was not stoichiometric. Metabolome studies revealed that this bacterium produces fluorinated anabolites and phospholipids. Mass spectrometric fatty acid profiling detected fluorinated long-chain (i.e., C_{12}−C_{19}) fatty acids in strain 273 cells grown with FD or DFD, and lipidomic profiling determined that 7.5 ± 0.2 and 82.0 ± 1.0% of the total phospholipids in strain 273 grown with FD or DFD, respectively, were fluorinated. The detection of the fluorinated metabolites and macromolecules represents a heretofore unrecognized sink for organofluorine, an observation with consequences for the environmental fate and transport of fluorinated aliphatic compounds.

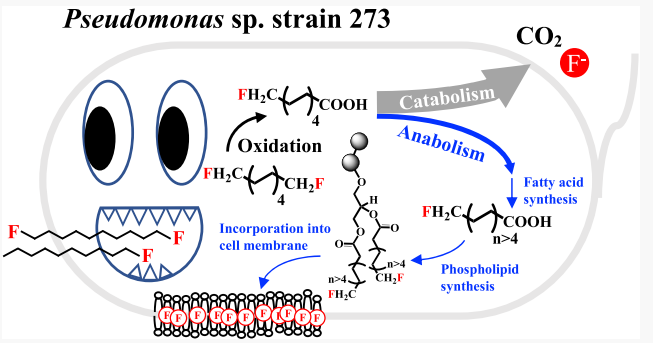

KEYWORDS: *fluorinated alkanes, lipid metabolism, lipidomics, fluorinated lipids, environmental fate*

INTRODUCTION

Synthetic organofluorine compounds have become of interest due to their unique physicochemical and biological properties and are produced for industrial, military, medical, and agrochemical applications.[1−4] This wide-ranging use has introduced organofluorine compounds into soil, groundwater, surface water, and air.[5,6] Particularly troublesome are recalcitrant per- and polyfluoroalkyl substances (PFAS), which have emerged as global contaminants linked to metabolic disruption, obesity, diabetes, immune suppression, and cancer in humans.[7−9] A major source of PFAS stems from the application of aqueous film-forming foam (AFFF) for fire suppression.[10−12] The recognition of PFAS recalcitrance triggered a transition to shorter chain length fluorinated compounds; however, replacement with environmentally benign compounds has not yet been accomplished.[13] The widespread use, recalcitrance, and potential negative human health effects of synthetic PFAS and other organofluorine compounds demand a detailed understanding of the fate of these chemicals and their transformation products in the environment.

The strength of the carbon−fluorine σ-bond is often used to explain why fluorinated chemicals are generally recalcitrant to (bio)degradation. Compared to the rich body of literature demonstrating biological dechlorination, reports of defluorinating microorganisms and defluorinating enzyme systems are limited.[14−16] Still, microbial degradation and enzymatic conversion of organofluorine compounds to nonfluorinated products have been demonstrated, illustrating that biological carbon−fluorine bond cleavage at neutral pH and at room temperature is feasible.[17] For example, *Pseudomonas* sp. strain 273 is an alkane degrader with the unique capability of degrading terminally monofluorinated and α,ω-bis-fluorinated medium-chain alkanes, including 1-fluorodecane (FD) and 1,10-difluorodecane (DFD), under oxic conditions.[18,19] Recent work suggested that a specialized bacterium can break carbon−carbon and carbon−fluorine bonds of perfluorooctanoic acid (PFOA) and perfluorooctanesulfonic acid (PFOS).[20] Although the relevance of these laboratory observations for in situ degradation and the longevity of organofluorine compounds in environmental systems remains uncertain, it adds to the mounting evidence that naturally occurring microbes can break carbon−fluorine σ-bonds.[16,21,22] Because robust microbial transformation and degradation processes for PFAS have not (yet) been described, current research and technology

Received: February 28, 2022
Revised: April 26, 2022
Accepted: May 4, 2022
Published: June 1, 2022

development efforts have a strong focus on aggressive physical−chemical treatment options.[23,24] Such processes can lead to the formation of products with a lower degree of fluorination, including terminally fluorinated alkanes, that could be more susceptible to microbial metabolism (e.g., by *Pseudomonas* sp. strain 273).

To advance the understanding of microbial degradation of organofluorine compounds, the metabolism of FD and DFD by the soil isolate *Pseudomonas* sp. strain 273 was studied.[19] In cultures that had completely consumed FD or DFD, a discrepancy between the theoretical and actual recovery of inorganic fluoride was noted. Efforts to determine the fate of the missing fluorine revealed the covalent incorporation of this element into long-chain fatty acids (FAs) and phospholipids. The observations have implications for understanding and monitoring the fate of organofluorine compounds in the environment and in biota, including humans.

MATERIALS AND METHODS

Chemicals. FD (purity >97%) was obtained from SynQuest Labs, Inc. (Alachua, FL). DFD (>97%) was custom-synthesized (Carbosynth, Newbury, UK). Sodium fluoride, sodium acetate, chloroform (>99.8%) and standards of fatty acid methyl esters were obtained from Sigma-Aldrich (St. Louis, MO). *n*-Decane (decane) was obtained from Acros Organics (Fair Lawn, NJ). Monofluoroacetate (MFA) was obtained from MP Biomedicals (Solon, OH). Phospholipid standards were obtained from Avanti Polar Lipids, Inc. (Alabaster, AL). Acetonitrile, ethanol, diethyl ether, pyridine, ammonium hydroxide, and methanol were obtained from Thermo Fisher Scientific (Waltham, MA). All other chemicals used were analytical reagent grade or higher.

Cultivation of *Pseudomonas* sp. Strain 273. Cultivation of *Pseudomonas* sp. strain 273 used a defined, phosphate-buffered (pH 7.3) mineral salt medium amended with different organic substrates, including decane, FD, or DFD, as the sole carbon sources.[19] The 160 mL glass serum bottles with 50 mL of medium and 110 mL air headspace were closed with butyl rubber stoppers (Bellco Glass Inc., Vineland, NJ) held in place with aluminum crimps. Experiments were initiated with cultures that had been transferred at least three times on the respective carbon substrate (1% inoculum, v/v). All culture bottles were incubated in an upright position at 30 °C and shaken at 120 rpm. For the metabolite analysis, quadruplicate vessels received decane, FD, or DFD (7 mM, nominal). To ensure sufficient supply of oxygen, the headspace volumes were replaced daily with air. Following a 4-day incubation period, the cells were harvested by centrifugation (8,000 × *g*, 15 min, room temperature) for extraction of FAs and lipids (Figure S3). To test for a possible *de novo* formation of C−F bonds, cultures were grown with 7 mM (nominal) decane in the presence of 2 mM fluoride. Strain 273 was also grown in medium with 7 mM (nominal) decane as the primary substrate and 2 mM MFA.

Fluoride Analysis. Fluoride ions were quantified with a Dionex ICS-2100 ion chromatograph equipped with a 4 mm × 250 mm IonPac AS18 hydroxide-selective anion-exchange column, a Dionex potassium hydroxide eluent generator cartridge, and a conductivity detector.[19] The system was operated at a flow rate of 1 mL min^{-1}.

To determine the recovery of inorganic fluoride during growth with fluoroalkanes, quadruplicate strain 273 cultures were grown in 160 mL glass serum bottles containing 10 mL of medium. The initial amount of neat (i.e., undiluted) fluoroalkane was determined gravimetrically, and 11.2 ± 0.1 mg of FD and 12.5 ± 0.1 mg of DFD were added to each vessel, resulting in initial nominal concentrations of 6.99 ± 0.05 and 6.98 ± 0.07 mM, respectively. A strain 273 culture grown with decane served as inoculum (1%, v/v) to avoid the introduction of inorganic fluoride. To ensure that oxygen was not limiting fluoroalkane degradation, 150 mL of air was injected by syringe (~2 atm). This amount of oxygen (~2.6 mmol) was in about 2.5-fold excess of the theoretical requirement for complete oxidation of the 70 μmol of fluoroalkane provided. To ensure complete fluoroalkane oxidation, the incubation vessels were briefly vented after 7 and 14 days before 2 atm air overpressure was applied. Live cultures quickly emulsified C_{10} alkanes, presumably via the production of a biosurfactant, and neither compound was detected in the headspace of the incubation vessels (100 μL direct injection, see below). Following a 3-week incubation period, no FD or DFD was detected in the medium, indicating complete consumption, and inorganic fluoride was analyzed.

(Fluoro)Decane Analysis. Decane, FD, and DFD were measured in hexane extracts using an Agilent 7890A gas chromatography-mass spectrometry (GC-MS) system (Agilent, Santa Clara, CA) equipped with an autosampler, a DB-624 column, and a mass-selective detector, as described.[19] The detection limits for decane, FD, and DFD were 2, 3, and 5 μM, respectively.

Fatty Acid (FA) Extraction and Derivatization. Biomass was collected from 10 mL culture suspensions by centrifugation at 8,000 × *g* for 15 min at room temperature. Following the removal of the supernatant, the cell pellets were immediately stored at −80 °C. Cellular FAs were extracted as described.[19,25] Briefly, the cells were lysed and saponified upon addition of an alkaline methanol solution and heated in a boiling water bath for 30 min. Then the cellular FAs were derivatized to fatty acid methyl esters in acidic methanol and extracted with hexanes.

Phospholipid Extraction. Cell pellets were collected from 10 mL of culture suspension as described above, and phospholipids were extracted following an established protocol with slight modifications.[26] The cell pellets were washed once with sterile mineral salt medium before 1 mL of extraction solvent composed of ethanol, Milli-Q water, diethyl ether, pyridine, and 4.2 M ammonium hydroxide (15:15:5:1:0.8, v/v), and 100 μL of acid-washed glass beads (diameter 150−212 μm, approximately 42,000 beads mL^{-1}, Sigma, St. Louis, MO) was added. The 1.5 mL plastic tubes (Eppendorf, Hamburg, Germany) were rigorously vortexed for 20 s, incubated in a water bath at 60 °C for 20 min, and centrifuged at 9600 × *g* for 10 min at room temperature. The upper organic layer of each tube was transferred to a new plastic tube, and the extraction was repeated twice. The combined organic layers were removed using a SpeedVac vacuum concentrator (ISS110−115 Integrated, Thermo Fisher Scientific) at 43 °C. The dried lipid extracts were stored at −80 °C. Prior to analysis, samples were suspended in 300 μL of methanol:chloroform (9:1, v/v).

Enumeration of Cells with Quantitative PCR (qPCR). Culture suspension samples (1 mL) were passed through 0.22 μm polyvinylidene difluoride membrane filters (Merck Millipore Ltd., Burlington, MA) to collect biomass for qPCR analysis. Genomic DNA was extracted from the cells on the membrane filters using the DNeasy Powerlyzer PowerSoil Kit (Qiagen, Hilden, Germany) following the manufacturer's

https://doi.org/10.1021/acs.est.2c01454
Environ. Sci. Technol. 2022, 56, 8155−8166

Table 1. Fluorine Mass Balances in *Pseudomonas* sp. Strain 273 Cultures Grown with FD or DFD[a]

substrate	initial amount	total fluorine	fluoride released		unaccounted fluorine	
	mmol L^{-1}	mmol L^{-1}	mmol L^{-1}[b]	%[c]	mmol L^{-1}[d]	%[e]
FD	6.99 ± 0.05	6.99 ± 0.05	6.44 ± 0.12	92.2 ± 2.2	0.55 ± 0.16	7.8 ± 2.2
DFD	6.98 ± 0.07	13.97 ± 0.14	13.20 ± 0.40	94.5 ± 2.8	0.77 ± 0.39	5.5 ± 2.8

[a]The experimental data were generated using 160 mL glass serum bottles with 10 mL of medium. The data represent the averages and the standard deviations of four replicate cultures. [b]Inorganic fluoride concentrations were measured 3 weeks after inoculation when fluoroalkanes had been completely consumed. [c]fluoride released percentage(%) $= \frac{\text{fluoride released (mM)}}{\text{total fluorine(mM)}} \times 100$. [d]The amount of fluorine unaccounted for represents the difference between the total fluorine introduced with the fluorinated growth substrate and the total amount of inorganic fluoride released. [e] unaccounted fluorine percentage(%). $= \frac{\text{fluorine unaccounted(mM)}}{\text{total fluorine (mM)}} \times 100$

protocol. Strain 273 16S rRNA genes were quantified with qPCR, as described.[19,27] The cell abundances were calculated by dividing the 16S rRNA gene copy numbers by a factor of 5 to account for the five 16S rRNA genes per genome.

Fatty Acid Methyl Ester (FAME) Analysis. FAME analysis used a GC coupled to an Exactive Plus Orbitrap mass spectrometer (Thermo Fisher Scientific) with an atmospheric pressure chemical ionization (APCI) interface, following established procedures (see the Supporting Information for details).[28]

Lipidomics Analyses. Untargeted lipidomics was conducted following a previously reported method using a Dionex UltiMate 3000 Ultra High-Performance Liquid Chromatography (UHPLC) system (Sunnyvale, CA) equipped with a CORTECS HILIC column (2.7 μm 2.1 × 150 mm, Waters, Milford, MA) and an Q Exactive Orbitrap mass spectrometer (Thermo Fisher Scientific) (see the Supporting Information for details).[29] The selected lipids, PE(34:1) and PG(34:1), were subjected to targeted analysis to determine their fragmentation patterns. The mass spectrometer was operated using parallel reaction monitoring (PRM) in negative mode. Data were collected at a resolution of 17,500, an isolation window of 0.5 m/z, and a normalized collisional energy of 35, with an inclusion list for relevant for all fluorinated forms of PE(34:1) and PG(34:1) (Table S4).

Nomenclature of FAs and Phospholipids. Lipid species are described using the following nomenclature: HG(SC:U), where HG denotes the headgroup, SC the total carbons in the acyl side chain(s), and U the total number of unsaturations. If any of these chemical descriptors could not be annotated, they are designated as unknown (Ukn). In FA and phospholipid designations, the first number in the brackets represents the total number of carbons in the FA chain(s) without indication of branched or linear structure and the second number represents the total number of unsaturations without indication of position. Fluorinated FAs and lipids are annotated by adding the extension $-F_x$ (e.g., HG(SC:db)$-F_x$), where x is the number of fluorine atoms in the lipid.

Lipid Library and Annotation. A predicted mass library was created for 13 lipid classes (Table 2) to include all possible FA tails from C_4 to C_{20} with up to six fluorine incorporations per species. A spectral feature was classified as unknown (Ukn plus letter designation) if the retention time differed from others in the same lipid class but was detected within the 2 min window. If the m/z and/or fragmentation characteristics matched a known lipid class, the spectral feature was annotated as the identified lipid class but with an unknown acyl side chain. In cases where the m/z and/or the fragmentation pattern could not be matched to known classes, the lipid was classified as unknown. Furthermore, if the mass data for any of these unknown compounds predicted fluorine incorporation based on spectral patterns associated with the alkane substrate, the species maintained the fluorine (F_0, F_1, F_2) nomenclature. If the fluorine incorporation could not be predicted, the nomenclature F_{ukn} was used.

Data Processing and Analysis. RAW files generated by Xcalibur were converted to mzML, a universal format, using msconvert.[30] The converted files were then imported into MAVEN, and peak abundances were identified and integrated by matching m/z (±5 ppm) and retention time (±2 min) to the lipid library.[31] The results were then exported to Microsoft Excel, and features with less than 2.5-fold abundance differences relative to the blanks and detected in less than half of the replicates were removed. In the case of low abundance lipids, missing values were replaced by the averages of other replicates.[32] The abundance data represent the averages of three replicate strain 273 cultures. Area counts of peaks from each sample were normalized to the cell numbers determined by qPCR. Fold changes were calculated from the average normalized abundances of three replicates and compared to the decane-grown cultures. p-values were determined using the Student's t-test. Fold changes were clustered using Cluster 3.0 and visualized with Java TreeView.[33] The extracted ion chromatograms (EIC) and PRM results were analyzed and plotted with Xcalibur Qual Browser, Version 4.0.27.19. All data are presented in the manuscript or are available in the Supporting Information. Lipidomics data have been deposited to the EMBL-EBI MetaboLights database with the identifier MTBLS3893 (www.ebi.ac.uk/metabolights/MTBLS3893).

RESULTS

Unaccounted Fluorine in Strain 273 Cultures Grown with Fluoroalkanes. Following complete consumption of 6.99 ± 0.05 mM FD, 6.44 ± 0.12 mM of inorganic fluoride was measured in the medium (Table 1). Cultures that received 6.98 ± 0.07 mM of DFD released 13.20 ± 0.40 mM of inorganic fluoride. The mass balance indicated that 7.8 ± 2.2 and 5.5 ± 2.8% of the fluorine the cultures received as FD or DFD, respectively, were not accounted for as inorganic fluoride (Table 1). Independent experimental replication corroborated that inorganic fluoride concentrations were consistently lower than predicted based on the amounts of fluoroalkanes consumed, suggesting an unidentified sink for fluorine.

Lipidome Analyses. Untargeted lipidomics detected lipid species from nine of the 13 lipid classes contained in databases (Table 2). In strain 273 cells grown with decane, FD, or DFD, 134 unique lipid species (differentiated by headgroup, number

https://doi.org/10.1021/acs.est.2c01454
Environ. Sci. Technol. 2022, 56, 8155−8166

of carbons in acyl chain[s], and the unsaturation number) were distributed among eight glycerophospholipid (GP) classes, including phosphatidylethanolamine (PE; 38 species), phosphatidylglycerol (PG; 18 species), phosphatidylcholine (PC; 12 species), phosphatidylserine (PS; 7 species), phosphatidic acid (PA; 4 species), lysophosphatidylethanolamine (LPE; 13 species), lysophosphatidylglycerol (LPG; 12 species), and lysophosphatidylcholine (LPC; 6 species), as well as ceramides (Cer; 9 species), which are a class of sphingolipids (Table 2). No other sphingolipids were detected. A total of 15 lipid species displayed retention times, fragmentation patterns, and/or predicted chemical formulae outside of the accepted limits for known headgroups and could not be assigned to any of the 13 lipid classes (Table 2).

To determine the global changes in the lipid class composition among cultures grown with decane, FD, or DFD, the ion intensities for each of the detected 134 lipid species were normalized to strain 273 cell abundances measured with quantitative PCR (qPCR). Partial least-squares discriminant analysis (PLS-DA) using the species detected in the lipidome analysis clearly distinguished strain 273 cells grown with each of the different carbon sources with 50.8% of the variation in component 1 separating decane- and DFD-grown cells, while component 2 contained 14.6% of the variation and clearly differentiated FD- from decane-grown cells (Figure 1A). To probe the changes in the carbon backbone of the acyl tails, the 134 lipid species were grouped based on the headgroup, total number of acyl carbons, and unsaturation number, while fluorination was not considered. Using these criteria, most lipid species were detected under all three growth conditions. The highest number of unique lipid species, 13, was exclusively observed in cultures grown with DFD, and cultures grown with decane and FD shared 18 lipid species that were not detected in DFD-grown cultures (Figure 1B).

Among the nine lipid classes detected, PE accounted for ~22% of total lipids detected in cells grown with decane or FD, and this lipid class increased to ~50% in cells grown with DFD. PG accounted for ~67% of the total lipids measured in cells grown with either decane or FD, while the content of PG decreased to 31% in cells grown with DFD (Figure 1C). Under the growth conditions tested, PE and PG were the dominant phospholipid classes and accounted for 81−89% of the total phospholipids. Cells grown with DFD displayed a higher proportion of PC (~6%) compared to cells grown with decane (~1%) or FD (~2%). Although ion counts cannot provide absolute quantification due to small differences in ionization potential among phospholipid classes, these measurements allow generalized conclusions. Phospholipid abundance estimates showed that cultures grown with decane, FD, or DFD produced cell number normalized total ion counts of $(3.0 \pm 0.3) \times 10^8$, $(3.5 \pm 0.1) \times 10^8$, and $(2.6 \pm 0.7) \times 10^8$, respectively, suggesting that the total phospholipid mass remained relatively constant across the three different growth conditions (Table S1).

Alterations in relative abundances of lipid headgroups were not the only significant effect from the utilization of fluoroalkanes, and the composition of the FAs comprising the acyl tails also varied. Fold change differences of individual lipid species between FD vs decane-grown and DFD vs decane-grown cells were calculated, and a total of 94 lipid species exhibited a fold change of greater than 2 with p-value of less than 0.05 in cells grown with a fluorinated substrate compared to cells that received decane as the carbon source (Figure 1D). Relative decreases in abundances of lipid classes

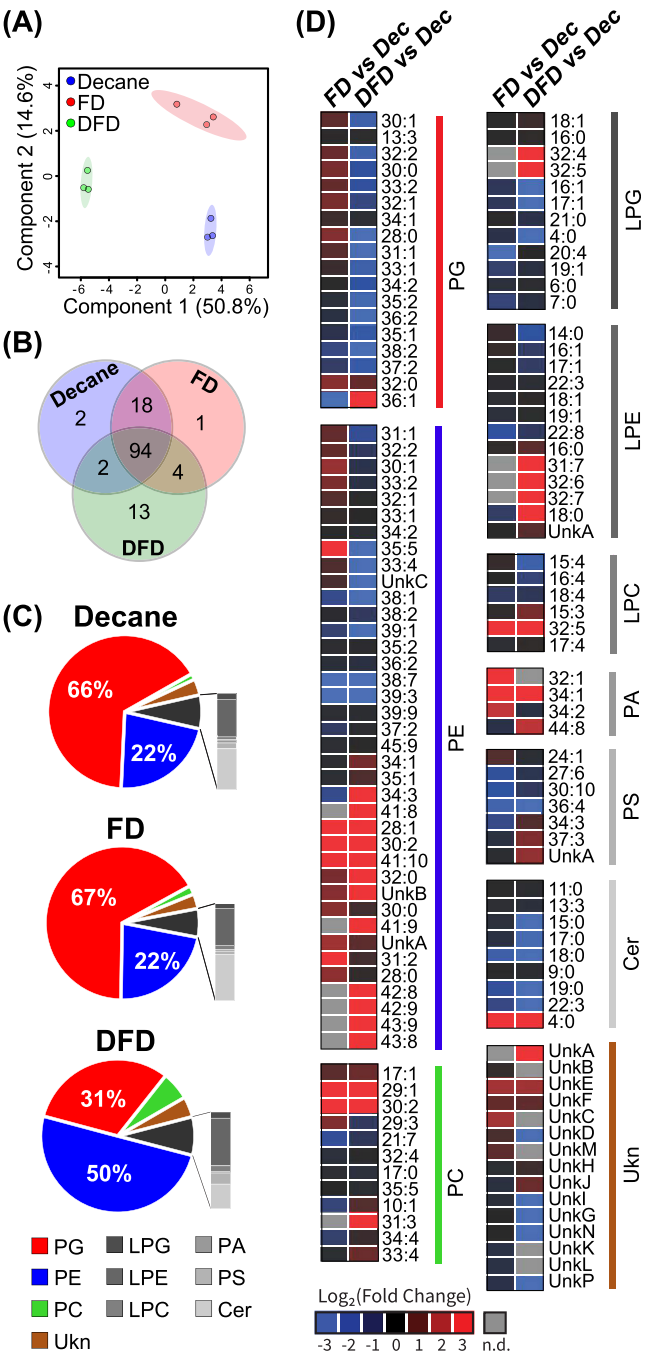

Figure 1. Lipidomic profiles of strain 273 cells grown with decane, fluorodecane, or difluorodecane. (A) Partial least-squares discriminant analysis (PLS-DA) of lipidomes of strain 273 cells grown with decane, FD, or DFD. Each point represents one of the three replicates. (B) Venn diagram showing the phospholipid species detected in strain 273 cells grown with different alkane substrates. (C) Abundances of all lipid species (summed fluorination states) per class measured in strain 273 cells grown with decane, FD, or DFD. (D) Heat map visualizing relative pool size changes between FD vs decane-grown and DFD vs decane-grown cells. An increase in fold change is indicated in red, and a decrease in fold change is indicated in blue. Fold changes are Log_2 transformed. Abbreviations: Decane (Dec), 1-fluorodecane (FD), 1,10-difluorodecane (DFD), and not detected (n.d.).

https://doi.org/10.1021/acs.est.2c01454
Environ. Sci. Technol. 2022, 56, 8155−8166

Table 2. Lipid Classes Used to Create the Phospholipid Database and Numbers of Fluorinated and Nonfluorinated Lipid Species Per Lipid Class/Headgroup[a]

lipid class/headgroup	abbreviation	number of species				unique species[c]
		F_0	F_1	F_2	F_{Ukn}	
phosphatidylglycerol	PG	18	16	15	0	18
phosphatidylethanolamine	PE	37	20	18	1	38
phosphatidylcholine	PC	9	7	5	0	12
phosphatidylserine	PS	7	3	3	0	7
phosphatidic acid	PA	4	3	2	0	4
lysophosphatidylglycerol	LPG	12	3	0	0	12
lysophosphatidylethanolamine	LPE	13	11	0	0	13
lysophosphatidylcholine	LPC	6	5	0	0	6
ceramides	Cer	9	3	0	0	9
unknown[b]	Ukn	4	4	4	11	15
phosphatidylinositol	PI	n.d.	n.d.	n.d.	n.d.	n.d.
phosphatidylinositol phosphate	PIP	n.d.	n.d.	n.d.	n.d.	n.d.
phosphatidylethanolamine sphingomyelin	SphingoPE	n.d.	n.d.	n.d.	n.d.	n.d.
phosphatidylcholine sphingomyelin	SphingoPC	n.d.	n.d.	n.d.	n.d.	n.d.
	TOTAL	119	75	47	12	134

[a]n.d. = not detected. [b]The category 'Unknown' includes spectral features whose lipid headgroup could not be identified. [c]Unique features determined from the summation of F_0, F_1, F_2, and F_{Ukn}. Some lipid species were only detected in their fluorinated forms.

were not indicative of a general decrease of all individual lipid species. For example, PG(32:0) and PG (36:1) increased in concentration in DFD-grown cells compared to decane-grown cells, while the total lipids comprising the PG class displayed a net decrease in relative abundance in these samples (Figure 1D).

Of all lipid species detected in strain 273, the majority (77−87%) contained 32 to 36 carbon atoms and ∼50% had one unsaturation in their two acyl tails under all three growth conditions. Lipids with >36 carbons made up ∼5% of lipids in cultures grown with DFD as compared to ∼1% in both decane- and FD-grown cells (Table 3). Also observed was a ∼5-fold

Table 3. Carbon Number and Unsaturations in Lipids Detected in *Pseudomonas* sp. Strain 273 Cells Grown with Decane, FD, or DFD[a]

carbon #	decane	FD	DFD
$<C_{32}$	8.3 ± 0.4%	9.8 ± 0.5%	11.5 ± 1.2%
C_{32}-C_{36}	86.8 ± 0.7%	86.2 ± 0.7%	77.5 ± 2.4%
$>C_{36}$	1.2 ± 0.1%	0.5 ± 0.05%	4.6 ± 0.6%
Ukn	3.7 ± 0.3%	3.6 ± 0.3%	6.3 ± 1.8%
# Unsaturation			
0	7.0 ± 0.3%	11.5 ± 0.6%	18.7 ± 3.4%
1	48.6 ± 0.5%	53.1 ± 1.0%	50.2 ± 0.9%
2	38.2 ± 0.8%	30.2 ± 1.0%	15.9 ± 1.1%
>2	2.5 ± 0.1%	1.6 ± 0.2%	8.8 ± 0.4%
Ukn	3.7 ± 0.3%	3.6 ± 0.3%	6.3 ± 1.8%

[a]Ukn = unknown.

increase in lipids with greater than 2 degrees of unsaturation, 8.8 ± 0.4% in DFD-grown cells versus 2.0 ± 0.5% in the other two growth conditions. Strain 273 cells grown with DFD further differentiated their lipids as they contained nearly double the amount of fully saturated lipids, 18.7 ± 3.4% versus 9.3 ± 0.5% in cells grown with decane or FD. Conversely, there was a ∼50% decrease in lipids with two unsaturations, 15.9 ± 1.1% in DFD-grown cells versus 34.2 ± 1.0% under the other two growth conditions (Table 3).

Detection of Covalently Bound Fluorine in Phospholipids. The lipidome analysis revealed PE and PG as the dominant lipid classes in strain 273 cells and suggested the presence of fluorine in a large percentage of these lipid species in DFD-grown cells (Figure 2). In both lipid classes, the 34:1 acyl chain was the most abundant species (Table S1). Due to the abundance of PE(34:1) and PG(34:1), these two species were chosen for further structural characterization to confirm the incorporation of fluorine. In cells grown with FD, 10.7 ± 0.5% of PE(34:1) and 5.5 ± 0.2% of PG(34:1) were detected with a single fluorine atom (F_1) incorporated. When DFD was the carbon source, the total fluorination increased to 94% for PE(34:1) with 45.5 ± 1.2% as F_1 and 48.9 ± 1.6% as F_2, and 88% for PG(34:1) with 53.8 ± 0.7% as F_1 and 34.1 ± 2.7% as F_2. The fragmentation pattern of PE(34:1) yielded $[M - H]^-$ fragments 255.2330, 281.2486, and 140.0118 m/z, which correspond to the 16:0 and 18:1 acyl chains and the characteristic ethanolamine phosphate headgroup fragment, respectively (Figure 3A,D). This observation was corroborated with fatty acid methyl ester (FAME) data that measured FA(16:0) and FA(18:1) (Figure 4).

In the fragments of the monofluorinated analogue PE (34:1)-F_1, the fragment ions representing ethanolamine phosphate, 16:0, 16:0-F_1 (273.2230 m/z), 18:1, and 18:1-F_1 (299.2386 m/z) were detected (Figure 3B,E). While the exact location of the fluorine cannot be determined from these data, only a single fluorine was detected per acyl side chain and was not detected on the headgroup fragment. Neither fluorinated phospholipids nor fluorinated fragments were detected in strain 273 grown with decane (Figure 3E). Fragmentation of bis-fluorinated PE(34:1)-F_2 yielded only fluorinated side chains 16:0-F_1 and 18:1-F_1 as well as the nonfluorinated ethanolamine phosphate headgroup (Figure 3C,F). This bis-fluorinated lipid species was only detected in strain 273 cells grown with DFD and not in cells grown with decane or FD, and only a single fluorine was detected in each acyl side chain. These findings are once again confirmed with the results from FAME analysis that measured FA(16:0)-F_1 and FA(18:1)-F_1 in strain 273 cells grown with FD or DFD (Figure 4). Fragmentation analyses of PG(34:1), PG(34:1)-F_1, and

https://doi.org/10.1021/acs.est.2c01454
Environ. Sci. Technol. 2022, 56, 8155−8166

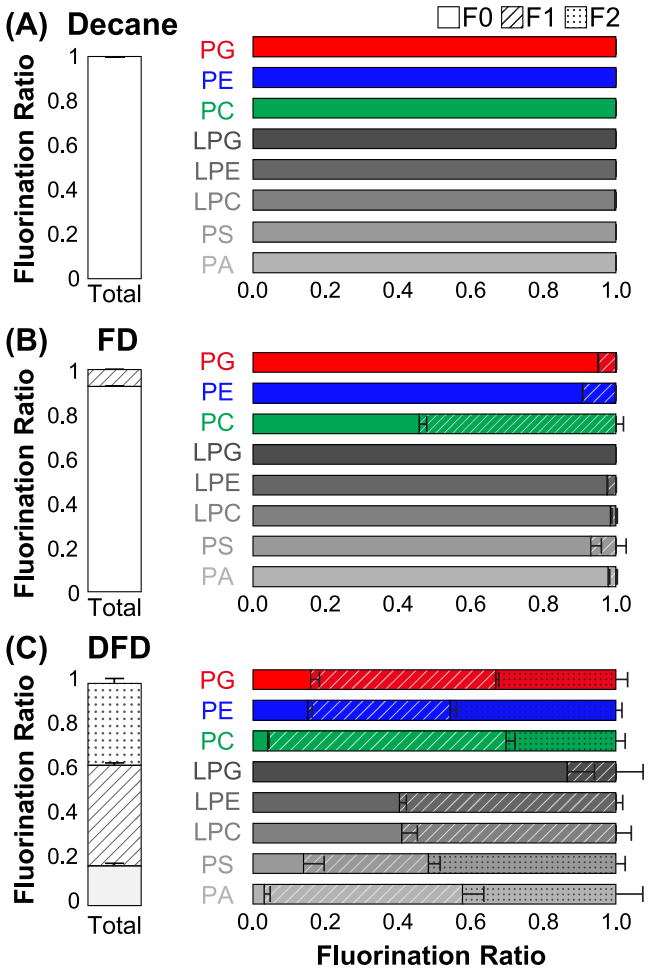

Figure 2. Percentages of fluorinated lipids in strain 273 cells grown with different carbon substrates. Bar graphs illustrating the percentages of total lipids (left panels) and individual lipid classes (right panels) with different degrees of fluorination (F_0, F_1, F_2) in strain 273 cells grown with (A) decane, (B) FD, or (C) DFD. Error bars represent the standard deviation of triplicate cultures. Note: Potentially fluorinated lipids with undetermined composition and/or extent of fluorination were removed from further fluorine incorporation calculations.

PG(34:2)-F_2 resulted in similar patterns across samples of strain 273 biomass grown with decane, FD, or DFD, respectively (Figure S1).

Detection of Fluorinated Long-Chain FAs. Targeted FAME analysis screening for 32 long-chain FAs showed that strain 273 cells grown with decane, FD, or DFD produced 11 FAs with >10 carbons. The FA pool in cells grown with decane was dominated by FA(16:0), FA(18:1), FA(16:1), FA(19:1), and FA(17:1), all nonfluorinated. The corresponding fluorinated analogues were detected in cultures grown with FD and were more abundant in cells grown with DFD (Figure 4). In total, seven monofluorinated FAs were detected in cells grown with FD or DFD (Table S2). Fluorinated FAs with more than a single fluorine substitution (i.e., $F_{>1}$) were not observed under any growth condition. Due to the varied ionization responses, quantitative comparison among FAs was not possible, and the relative abundances of a single ionization species under different growth conditions are shown in Figure 4 and Table S2.

Assimilation of Organofluorine into the Lipidome of Strain 273. Fluorinated lipids were exclusively detected in strain 273 cells grown with fluoroalkanes and were more abundant in cells grown with DFD than in cells grown with FD (Figure 2). Of the total phospholipid species detected, 75 contained one fluorine substitution (F_1) and 47 contained two fluorine substitutions (F_2) (Table 2). Approximately 7.5 ± 0.2 and 45.2 ± 1.0% of the total lipids contained a single fluorine when strain 273 was grown with FD or DFD, respectively, and the relative abundances of lipids with two fluorine substitutions were <0.1 and 36.8 ± 2.2%, respectively, in cells grown with FD versus DFD (Figure 2). Lipids with more than two fluorine substitutions (i.e., $F_{>2}$) were not detected in any cultures.

The eight GP classes (i.e., PG, PE, PC, PS, PA, LPG, LPE, and LPC) accounted for over 97% of the total lipids detected in strain 273 cells under all growth conditions, and the percentages of fluorinated lipids within individual GP classes were determined for both FD- and DFD-grown cells (Figure 2). In general, the percentage of GPs containing 1 or 2 fluorine substitution(s) was much higher in DFD- than in FD-grown cells, and ≥80% of the phospholipids in cells grown with DFD were fluorinated. Only a small portion of PE and PG species remained nonfluorinated in cells grown with DFD (Figure 2). About half (54%) of PC was fluorinated in cells grown with FD while less than 10% fluorination was observed in all other phospholipid classes. In DFD-grown cells, the majority (>86%) of the GPs, including PE, PG, PC, PS, and PA, were fluorinated (F_1 or F_2). In contrast, the majority of the PE and PG species in cells grown with FD were nonfluorinated (F_0) (Figure 2). A single fluorine was detected in three lysophospholipids, including LPE (59% F_1), LPC (60% F_1), and LPG (13% F_1) in strain 273 cells grown with DFD. Monofluorinated lysophospholipids did not exceed 2% in FD-grown cells (Figure 2), and bis-fluorinated lysophospholipids were not detected under any growth condition.

Strain 273 did not grow with monofluoroacetate (MFA) as the sole carbon source; however, co-metabolic consumption of MFA was observed in cultures with decane as a primary substrate. In strain 273 cells grown with 7 mM (nominal) decane in the presence of 2 mM MFA, 2.1 ± 0.1 and 2.0 ± 0.2% of PE and PG, respectively, were fluorinated. This finding demonstrates the assimilation of fluorine from MFA into lipids, although the percentage of species containing fluorine was lower compared to FD- or DFD-grown cells (Figure S2). All fluorinated lipid species detected in MFA/decane-grown cells were also detected in FD- or DFD-grown cells. Fluorinated GPs were detected exclusively in strain 273 cells when growth occurred in medium with FD, DFD, or MFA (with decane as the primary substrate). In cells grown with decane with decane in the presence of 2 mM fluoride, fluorinated GPs were not detected, suggesting the organism cannot form C−F bonds using inorganic fluoride under the growth conditions employed.

DISCUSSION

Lipid Composition in *Pseudomonas* sp. Strain 273. Consistent with its phylogenetic characterization, strain 273 shares similar lipid classes with other pseudomonads, with PE and PG accounting for the majority of the total phospholipids.[34−36] The GC-MS-based FAME analysis detected FAs with 16 and 18 carbon atoms, and the LC-MS-based lipidome analysis determined that 78−87% of the phospholipids in strain 273 contained 32 to 36 carbons in the two FA tails

https://doi.org/10.1021/acs.est.2c01454
Environ. Sci. Technol. 2022, 56, 8155−8166

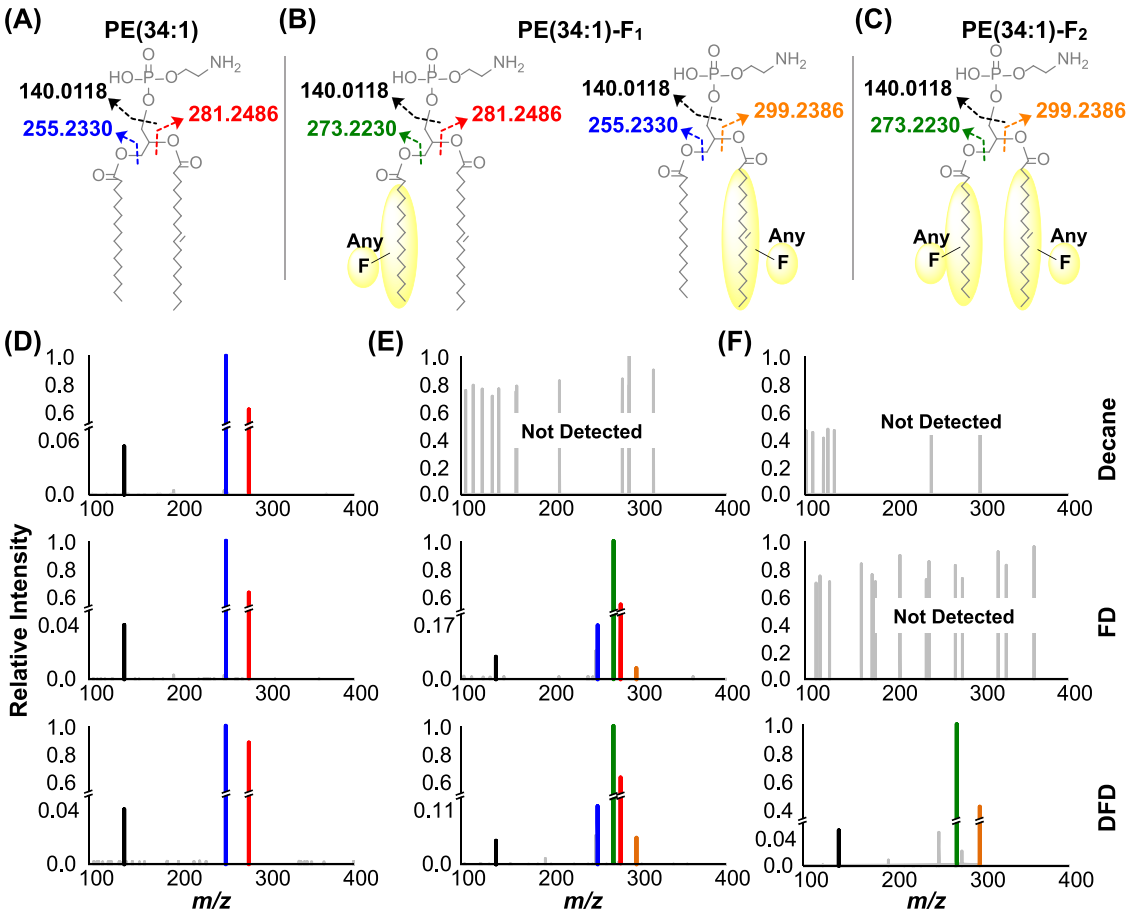

Figure 3. Identification of fluorinated phospholipids. Predicted fragmentations for PE(16:0/18:1) (A), PE(16:0-F_1/18:1) and PE(16:0/18:1-F_1) (B), and PE(16:0-F_1/18:1-F_1) (C) and the expected masses of the fragments for each species are depicted. Parent and fragment masses measured for PE(34:1) (D), PE(34:1)-F_1 (E), and PE(34:1)-F_2 (F) obtained from cultures grown with decane, FD, or DFD are shown. The peak colors denote the negatively charged fragment masses shown in panels A−C. Note: SN1 and SN2 positions on the lipid are arbitrarily assigned.

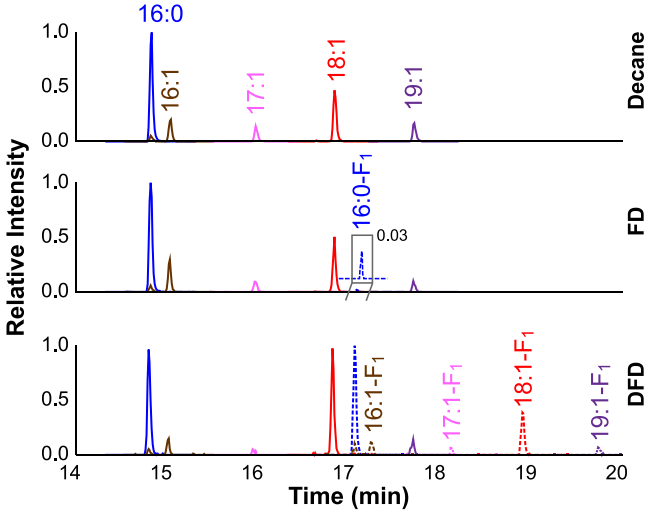

Figure 4. Long-chain FAs detected in strain 273 cells grown with decane, FD, or DFD. Illustrated are the combined extracted ion chromatograms (EICs) of the top-five abundant FAs and their fluorinated analogues detected. The most responsive ion of each FAME species is shown. The solid lines show long-chain, non-fluorinated FAs, and the dashed lines show their fluorinated analogues. The inset represents the magnified view of the EIC representing FA(16:0)-F_1.

combined. For comparison, >93% of membrane lipids from *Pseudomonas putida* grown with butanol contained tails with 16 or 18 carbon atoms.[34] Regardless of fluorine substitution, the phospholipid composition of strain 273 cells grown with decane, FD, or DFD was similar to that reported for other *Pseudomonas* spp.

Assimilation of (Organo)Halogens. Bacterial incorporation of organohalogens into lipids is not unprecedented, and the formation of iodinated, brominated, and chlorinated lipids has been observed in *Rhodococcus rhodochrous* strain NCIMB 13064.[37,38] During the growth of strain NCIMB 13064 with medium- to long-chain 1-chloro-, 1-bromo-, and 1-iodoalkanes, up to 75, 90, and 81%, respectively, of the total FAs were substituted in the ω-position with the corresponding halogen.[38] This strain was reported to grow with 1-fluorotetradecane without fluoride release, and FA(14:0)-F_1 was the only fluorinated FA detected in lipid extracts representing no more than 1% of the total FA content.[37,38] There is also evidence for de novo synthesis of C−F bonds. Bacterial formation of fluorometabolites has been observed in members of the *Actinobacteria* (i.e., *Streptomyces*, *Actinoplanes*, *Norcardia*) possessing fluorinases that convert *S*-adenosyl-L-methionine and inorganic fluoride to 5′-fluoro-5′-deoxyadenosine, which can subsequently be metabolized to fluorothreonine and MFA.[39,40] Fluorine metabolism is not restricted to the bacterial kingdom, and several ω-substituted monofluoro FAs have been found in the seeds of the shrub

https://doi.org/10.1021/acs.est.2c01454
Environ. Sci. Technol. 2022, 56, 8155−8166

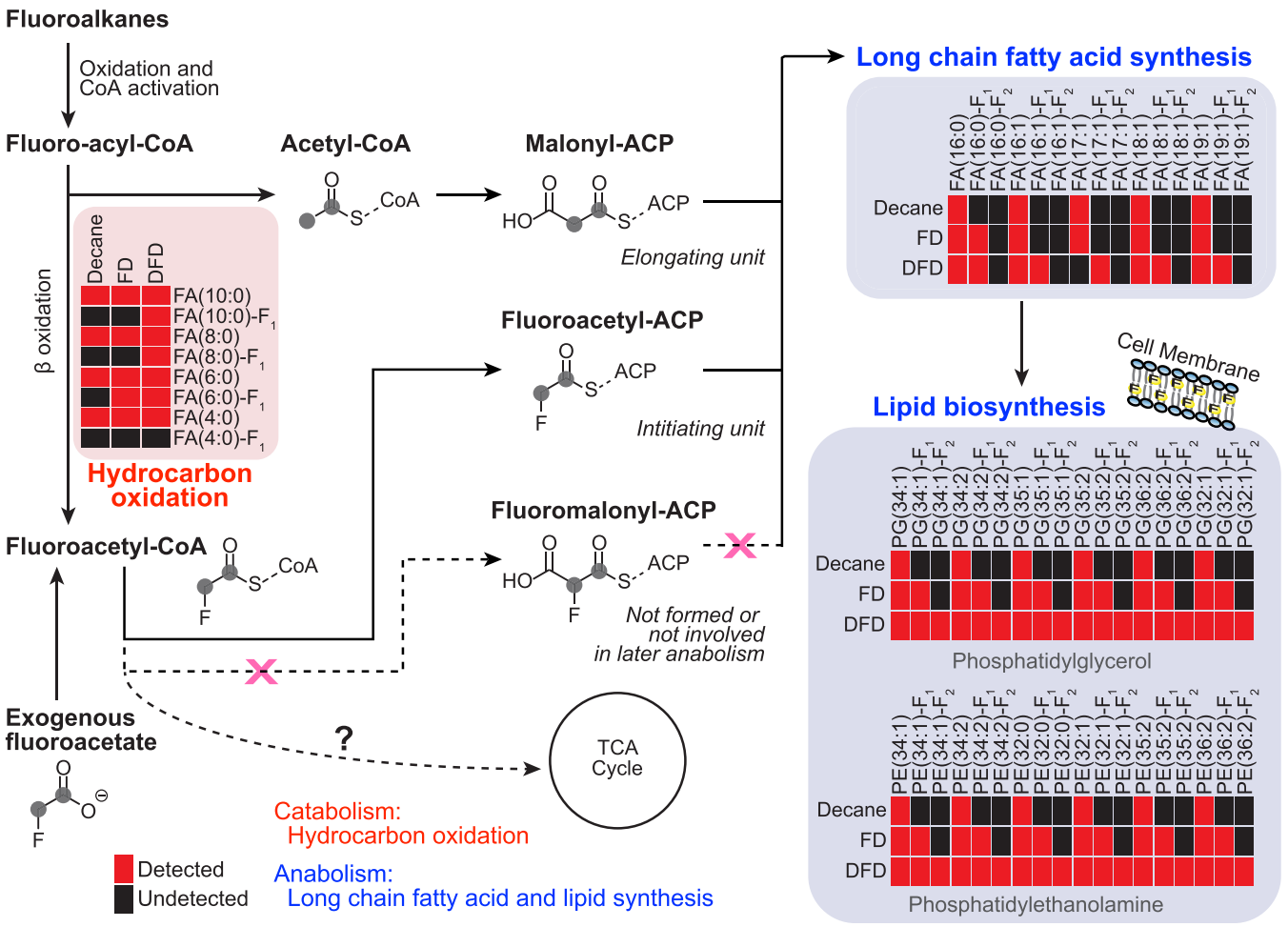

Figure 5. Proposed pathway for fluorine assimilation in *Pseudomonas* sp. strain 273. Metabolites experimentally identified in strain 273 cells grown with decane, FD, or DFD are indicated by red rectangles; the black rectangles indicate metabolites that were not detected. The closed gray circles in the chemical structures indicate carbon atoms assimilated into the FA chain in each iterative elongation cycle, each step associated with the consumption of one malonyl-ACP. The data illustrating hydrocarbon oxidation (red box) were adapted from a previous study.[19]

Dichapetalum toxicarium, which have noted toxicity as they can be catabolized via *β*-oxidation to form MFA.[41]

Metabolism of Fluorinated Alkanes. A previous study detected C_6, C_8, and C_{10} fluorinated FAs during the growth of strain 273 with FD and DFD, suggesting a catabolic route via *β*-oxidation resulting in the formation of *ω*-fluorofatty acyl-CoA catabolites.[19] The data herein demonstrate the formation of fluorinated FAs with carbon chain lengths greater than 10 (i.e., C_{12}−C_{19}), indicative of fluorinated FA elongation (Figure 5). Long-chain FAs detected in cells grown with fluoroalkanes contained a single fluorine substitution, and no evidence was obtained for FAs with multiple fluorine atoms. A plausible explanation is a catabolic route via *β*-oxidation leading to the formation of MFA-CoA, which could be used by the MFA-acyl carrier protein (ACP) and serve as the initiating unit in long-chain FA biosynthesis. In support of this hypothesis, fluorinated GPs were detected in cells grown with decane in the presence of MFA as the sole source of a fluoroalkyl moiety. Strain 273 does not grow with MFA but apparently can channel MFA into the FA anabolic pathway when a primary carbon substrate (e.g., decane) supports growth (i.e., co-metabolic utilization of MFA). In each iterative elongation cycle, two carbon atoms, with one of them potentially carrying a fluorine, are added to the fatty acyl-ACP (Figure 5). Polyfluorinated FAs were not detected, suggesting either an inability to convert MFA-CoA to fluoromalonyl-ACP, the exclusion of fluoromalonyl-ACP from acyl chain elongation, or a mechanism that eliminates secondary fluorines from lipid biosynthetic precursors, all of which would explain the formation of monofluorinated FAs only (Figure 5). These scenarios are consistent with the formation of FAs with terminal F substitution. Similar observations were made in the shrub *Dichapetalum cymosum* capable of *de novo* C−F bond formation and synthesis of *ω*-fluorinated but not polyfluorinated FAs.[41−43]

The manufacturers of FD and DFD indicated compound purities of >97%, and our analytical procedures did not detect any impurities. The significant difference in the abundance of fluorinated lipids in cells grown with FD versus DFD indicates that any potential contribution of organofluorine from impurities was negligible and without bearing on the results reported here. The percentage of fluorinated lipids in strain 273 cells grown with DFD was ∼11-fold higher than when grown with FD, suggesting that the monooxygenase preferentially attacks the fluorinated carbon of the alkane (i.e., a 2-fold difference in fluorination percentage would be expected if the attack was random). The observed assimilation of fluorine into GPs and ceramides suggests enzyme promiscuity in anabolic pathways, as strain 273 enzyme systems involved in long-chain FA and lipid biosynthesis do not apparently discriminate

https://doi.org/10.1021/acs.est.2c01454
Environ. Sci. Technol. 2022, 56, 8155−8166

between fluorinated and nonfluorinated metabolites. Such enzyme promiscuity is not unprecedented, and replacement of C−H with C−F has been noted to be the most conservative steric replacement for H, likely due to a combination of the relatively modest atomic radius of F combined with the short C−F bond distance.[44] For instance, *Escherichia coli* adapted to utilize fluorinated precursors (i.e., fluoroindole) produced fluorotryptophan rather than tryptophan and assimilated the fluorinated amino acid into the cellular proteome.[45]

Potential Impact of Fluorination on Membrane Functionality. The phospholipid membrane composition impacts the cell membrane fluidity and permeability and is responsive to stressors;[46,47] however, the impact of fluorination on the functionality of the cellular membrane is uncertain. The artificial assembly of a GP bilayer comprising 1-palmitoyl-2-[16-fluoropalmitoyl]-phosphatidylcholine (F-DPPC), which has one FA tail with a terminal fluorine substitution, preferentially formed interdigitated layers at the gel phase, causing the membrane phase transition temperature to increase by 10 °C compared to a bilayer with the nonfluorinated analogue.[48] *In vivo* studies with *E. coli* strain K1060B5 demonstrated that up to 50 mol % of exogenously supplied geminal difluoromethylene FAs (i.e., 8,8-difluoromyristic acid) could be incorporated into membrane phospholipid tails.[49] Altered lipid/protein ratios, modified cross-membrane transport characteristics, and reduced growth rates were observed when 20 mol % of FAs in cells of strain K1060B5 were fluorinated.[50] Conversely, *Acholeplasma laidlawii* strain B can incorporate up to 80 mol % of synthetic monofluorinated palmitic acid into the membrane without apparent effects on lipid/protein ratios and growth yields.[51,52] In strain 273 cells, up to 82% of the total phospholipids were fluorinated when cells utilized DFD as a carbon substrate, and the culture could be repeatedly transferred in medium with DFD as the sole carbon source. The increased abundance of polyunsaturated phospholipids and elevated PE content in highly fluorinated strain 273 lipidomes following growth with DFD could be compensatory mechanisms against stress induced by fluorine incorporation into the lipids.[53] More detailed studies are warranted to explore the consequences of fluorine incorporation for membrane functionality.

Anabolite Pool and the Lipid Bilayer as Unrecognized Sinks for Organofluorine. Studies to date have focused on measuring organofluorine compounds in environmental matrices (e.g., groundwater, soil, sediment, aquifer material, sludge, landfill leachate) as well as in tissue and blood samples of animals and humans. Bioaccumulation (and in some cases, biomagnification) of organofluorine compounds (e.g., certain PFAS) has been demonstrated in plants,[54] animals,[55] and humans.[56−58] A positive correlation between phospholipid levels and PFAS concentrations was observed in different organs of North Atlantic pilot whales.[59] A recent study demonstrated a noncovalent association of PFAS with the bacterial lipid bilayer of a Gram-positive (*Staphylococcus epidermidis*) and a Gram-negative (*Aliivibrio fischeri*) bacterium.[60] No significant differences in terms of PFAS accumulation existed in live versus dead cells, indicative of a passive and reversible process driven by hydrophobic and electrostatic interactions. The current study reports a different process leading to the covalent incorporation of fluoroalkyl moieties into the bacterial membrane and reveals a novel, heretofore unrecognized sink for organofluorine through anabolic routes (i.e., biosynthesis of fluorinated FAs and fluorinated lipids). The experimental efforts with strain 273 demonstrated that 82% of the total phospholipids contained fluorine, 45% as F_1, and 37% as F_2, following growth with DFD. Based on the generic number of 2.2×10^7 GP molecules per cell (i.e., 3.7×10^{-17} mol cell^{-1}),[61] we calculate that a single cell incorporated 4.35×10^{-11} μmol of fluorine. qPCR analysis determined that cultures receiving 7 mmol L^{-1} DFD produced $(1.12 \pm 0.05) \times 10^9$ cells mL^{-1} (Table S3). Thus, fluorine incorporation into phospholipids accounted for approximately 50 μmol L^{-1}. The assimilation of fluorine into the lipid bilayer and potentially other cellular macromolecules (e.g., proteins), represents a heretofore unrecognized sink for organofluorine, a finding with an impact for the fate and transport of fluorinated chemicals in the environment. The fate of the fluorinated lipids following cell death or predation is unclear, but it is likely that other microorganisms utilize fluorinated metabolites for anabolic purposes. In such a scenario, more widespread fluorine incorporation into microbial biomass would be predicted in environments impacted by organofluorine compounds. Considering that 1 g of soil (dry weight) harbors 1.5×10^{10} bacterial cells,[62] microbial biomass represents a sizable sink, and source, of organofluorine, with potential for trophic magnification through food chains.

The extent to which eukaryotic cells incorporate organofluorine via anabolic routes is unclear; however, the incorporation of α-fluoropalmitic acid into the phospholipids of cultured BALB/C mouse embryo cell lines suggests this can occur.[63] PFAS have been detected and quantified in various mammal species, including humans.[56−58] Following solvent extraction of organofluorine and subsequent analysis of PFAS in mammalian tissue or blood samples, differences between the total organofluorine (determined as fluoride by combustion ion chromatography) and measurable organofluorine compounds (e.g., PFAS measured by LC-MS) were reported.[64−66] These observations hint at unidentified reservoirs of organofluorine compounds in mammals, and the incorporation of fluorine into cellular macromolecules via anabolic routes, as described here for a bacterium, seems plausible and should be explored further.

■ ASSOCIATED CONTENT

Supporting Information

The Supporting Information is available free of charge at https://pubs.acs.org/doi/10.1021/acs.est.2c01454.

Phospholipid abundances in strain 273 cells grown with decane, FD, or DFD (Table S1); FAME abundances in strain 273 cells grown with decane, FD, or DFD (Table S2); cell abundances in cultures of strain 273 grown with different carbon sources (Table S3); inclusion list for parallel reaction monitoring analysis of PE(34:1), PG(34:1), and their fluorinated analogues (Table S4) (XLSX)

Experimental procedures detailing FAME and lipidomics analyses; Identification of fluorinated phospholipids (Figure S1); the detection of PE(34:1)-F1 in cells of strain 273 grown with different carbon sources (Figure S2); schematic of the experimental study design (Figure S3) (PDF)

https://doi.org/10.1021/acs.est.2c01454
Environ. Sci. Technol. 2022, 56, 8155−8166

AUTHOR INFORMATION

Corresponding Authors

Shawn R. Campagna − *Department of Chemistry and Biological and Small Molecule Mass Spectrometry Core, University of Tennessee, Knoxville, Tennessee 37996, United States; University of Tennessee - Oak Ridge Innovation Institute, Knoxville, Tennessee 37996, United States;* orcid.org/0000-0001-6809-3862; Email: campagna@utk.edu

Frank E. Löffler − *Department of Civil and Environmental Engineering, University of Tennessee, Knoxville, Tennessee 37996, United States; Center for Environmental Biotechnology, Department of Microbiology, and Department of Biosystems Engineering and Soil Science, University of Tennessee, Knoxville, Tennessee 37996, United States; Biosciences Division, Oak Ridge National Laboratory, Oak Ridge, Tennessee 37831, United States;* orcid.org/0000-0002-9797-4279; Email: frank.loeffler@utk.edu

Authors

Yongchao Xie − *Department of Civil and Environmental Engineering, University of Tennessee, Knoxville, Tennessee 37996, United States; Center for Environmental Biotechnology, University of Tennessee, Knoxville, Tennessee 37996, United States;* Present Address: Department of Chemistry and Biochemistry, University of California, Los Angeles, California 90095, United States

Amanda L. May − *Center for Environmental Biotechnology, University of Tennessee, Knoxville, Tennessee 37996, United States*

Gao Chen − *Department of Civil and Environmental Engineering, University of Tennessee, Knoxville, Tennessee 37996, United States; Center for Environmental Biotechnology, University of Tennessee, Knoxville, Tennessee 37996, United States;* orcid.org/0000-0002-8767-3130

Lindsay P. Brown − *Department of Chemistry, University of Tennessee, Knoxville, Tennessee 37996, United States*

Joshua B. Powers − *Department of Chemistry, University of Tennessee, Knoxville, Tennessee 37996, United States*

Eric D. Tague − *Department of Chemistry, University of Tennessee, Knoxville, Tennessee 37996, United States;* orcid.org/0000-0001-8031-4816

Complete contact information is available at: https://pubs.acs.org/10.1021/acs.est.2c01454

Author Contributions

Y.X. and F.E.L. conceptualized the study; Y.X., E.D.T., S.R.C., and F.E.L. designed experiments; Y.X. performed the laboratory experiments; G.C. provided laboratory expertise and assistance; A.L.M. and Y.X. performed the lipidome analyses with contributions from L.P.B., J.B.P., E.D.T. and S.R.C.; Y.X., A.L.M, S.R.C. and F.E.L. interpreted results; Y.X. and A.L.M visualized data; Y.X., A.L.M., S.R.C, and F.E.L. wrote the paper. All authors provided input and edits to the final manuscript.

Notes

The authors declare no competing financial interest.

ACKNOWLEDGMENTS

This work was supported by The University Consortium for Field-Focused Groundwater Research. The authors acknowledge support from the China Scholarship Council to YX during his study at the University of Tennessee, Knoxville. Support for the analytical work was from NSF Award MCB-1615373 to JBP, NIH/NIAID Award R01AI116571 to EDF, and the University of Tennessee−Oak Ridge Innovation Institute (UT-ORII) for providing a fellowship to LPB. Some of the analyses used instrumentation provided by NSF Award DBI-1530975. The authors thank the Biological and Small Molecule Mass Spectrometry Core at the University of Tennessee (RRID: SCR_021368) for sample processing and data collection as well as H. Castro for assistance and helpful discussions.

REFERENCES

(1) Müller, K.; Faeh, C.; Diederich, F. Fluorine in pharmaceuticals: looking beyond intuition. *Science* **2007**, *317*, 1881−1886.

(2) Theodoridis, G. Fluorine-containing agrochemicals: an overview of recent developments. In *Fluorine and the Environment Agrochemicals, Archaeology, Green Chemistry & Water*, Tressaud, A., Ed.; Elsevier, 2006; Vol. 2, pp 121−175.

(3) Fujiwara, T.; O'Hagan, D. Successful fluorine-containing herbicide agrochemicals. *J. Fluorine Chem.* **2014**, *167*, 16−29.

(4) Inoue, M.; Sumii, Y.; Shibata, N. Contribution of organofluorine compounds to pharmaceuticals. *ACS Omega* **2020**, *5*, 10633−10640.

(5) Maienfisch, P.; Hall, R. G. The importance of fluorine in the life science industry. *Chimia* **2004**, *58*, 93−99.

(6) Glüge, J.; Scheringer, M.; Cousins, I. T.; DeWitt, J. C.; Goldenman, G.; Herzke, D.; Lohmann, R.; Ng, C. A.; Trier, X.; Wang, Z. An overview of the uses of per-and polyfluoroalkyl substances (PFAS). *Environ. Sci.: Processes Impacts* **2020**, *22*, 2345−2373.

(7) Grandjean, P.; Heilmann, C.; Weihe, P.; Nielsen, F.; Mogensen, U. B.; Timmermann, A.; Budtz-Jørgensen, E. Estimated exposures to perfluorinated compounds in infancy predict attenuated vaccine antibody concentrations at age 5-years. *J. Immunotoxicol.* **2017**, *14*, 188−195.

(8) Sun, Q.; Zong, G.; Valvi, D.; Nielsen, F.; Coull, B.; Grandjean, P. Plasma concentrations of perfluoroalkyl substances and risk of type 2 diabetes: a prospective investigation among US women. *Environ. Health Perspect.* **2018**, *126*, No. 037001.

(9) Liu, G.; Dhana, K.; Furtado, J. D.; Rood, J.; Zong, G.; Liang, L.; Qi, L.; Bray, G. A.; DeJonge, L.; Coull, B.; et al.*et al.* Perfluoroalkyl substances and changes in body weight and resting metabolic rate in response to weight-loss diets: a prospective study. *PLoS Med.* **2018**, *15*, No. e1002502.

(10) Houtz, E. F.; Higgins, C. P.; Field, J. A.; Sedlak, D. L. Persistence of perfluoroalkyl acid precursors in AFFF-impacted groundwater and soil. *Environ. Sci. Technol.* **2013**, *47*, 8187−8195.

(11) Barzen-Hanson, K. A.; Roberts, S. C.; Choyke, S.; Oetjen, K.; McAlees, A.; Riddell, N.; McCrindle, R.; Ferguson, P. L.; Higgins, C. P.; Field, J. A. Discovery of 40 classes of per-and polyfluoroalkyl substances in historical aqueous film-forming foams (AFFFs) and AFFF-impacted groundwater. *Environ. Sci. Technol.* **2017**, *51*, 2047−2057.

(12) Nickerson, A.; Maizel, A. C.; Kulkarni, P. R.; Adamson, D. T.; Kornuc, J. J.; Higgins, C. P. Enhanced extraction of AFFF-associated PFASs from source zone soils. *Environ. Sci. Technol.* **2020**, *54*, 4952−4962.

(13) Brendel, S.; Fetter, É.; Staude, C.; Vierke, L.; Biegel-Engler, A. Short-chain perfluoroalkyl acids: environmental concerns and a regulatory strategy under REACH. *Environ. Sci. Eur.* **2018**, *30*, No. 9.

(14) Goldman, P. The enzymatic cleavage of the carbon-fluorine bond in fluoroacetate. *J. Biol. Chem.* **1965**, *240*, 3434−3438.

(15) Liu, J.-Q.; Kurihara, T.; Ichiyama, S.; Miyagi, M.; Tsunasawa, S.; Kawasaki, H.; Soda, K.; Esaki, N. Reaction mechanism of fluoroacetate dehalogenase from *Moraxella* sp. B. *J. Biol. Chem.* **1998**, *273*, 30897−30902.

(16) Liu, J.; Avendaño, S. M. Microbial degradation of polyfluoroalkyl chemicals in the environment: a review. *Environ. Int.* **2013**, *61*, 98−114.

(17) Lim, X. *Can Microbes Save us from PFAS?*; 2374-7943; ACS Publications, 2021; pp 3−6.
(18) Wischnak, C.; Löffler, F. E.; Li, J.; Urbance, J. W.; Müller, R. *Pseudomonas* sp. strain 273, an aerobic α, ω-dichloroalkane-degrading bacterium. *Appl. Environ. Microbiol.* **1998**, *64*, 3507−3511.
(19) Xie, Y.; Chen, G.; May, A. L.; Yan, J.; Brown, L. P.; Powers, J. B.; Campagna, S. R.; Löffler, F. E. *Pseudomonas* sp. strain 273 degrades fluorinated alkanes. *Environ. Sci. Technol.* **2020**, *54*, 14994−15003.
(20) Huang, S.; Jaffé, P. R. Defluorination of perfluorooctanoic acid (PFOA) and perfluorooctane sulfonate (PFOS) by *Acidimicrobium* sp. strain A6. *Environ. Sci. Technol.* **2019**, *53*, 11410−11419.
(21) Yu, Y.; Zhang, K.; Li, Z.; Ren, C.; Chen, J.; Lin, Y.-H.; Liu, J.; Men, Y. Microbial cleavage of C−F bonds in two C_6 per-and polyfluorinated compounds via reductive defluorination. *Environ. Sci. Technol.* **2020**, *54*, 14393−14402.
(22) Wackett, L. P. Nothing lasts forever: understanding microbial biodegradation of polyfluorinated compounds and perfluorinated alkyl substances. *Microbiol. Biotechnol.* **2022**, *15*, 773−792.
(23) Bentel, M. J.; Yu, Y.; Xu, L.; Li, Z.; Wong, B. M.; Men, Y.; Liu, J. Defluorination of per- and polyfluoroalkyl substances (PFASs) with hydrated electrons: structural dependence and implications to PFAS remediation and management. *Environ. Sci. Technol.* **2019**, *53*, 3718−3728.
(24) Cui, J.; Gao, P.; Deng, Y. Destruction of per-and polyfluoroalkyl substances (PFAS) with advanced reduction processes (ARPs): A critical review. *Environ. Sci. Technol.* **2020**, *54*, 3752−3766.
(25) Sasser, M. *Bacterial Identification by Gas Chromatographic Analysis of Fatty Acids Methyl Esters (GC-FAME)*, Microbial IDentification Inc.: In Newark, NY, 2006; pp http://midi-inc.com/pdf/MIS_Technote_101.pdf.
(26) Guan, X. L.; Riezman, I.; Wenk, M. R.; Riezman, H. Yeast lipid analysis and quantification by mass spectrometry. In *Methods in Enzymology*,Abelson, J. N.; Simon, M. I., Eds.; Elsevier: San Diego, CA, 2010; Vol. *470*, pp 369−391.
(27) Ritalahti, K. M.; Amos, B. K.; Sung, Y.; Wu, Q.; Koenigsberg, S. S.; Löffler, F. E. Quantitative PCR targeting 16S rRNA and reductive dehalogenase genes simultaneously monitors multiple *Dehalococcoides* strains. *Appl. Environ. Microbiol.* **2006**, *72*, 2765−2774.
(28) Powers, J. B.; Campagna, S. R. Design and evaluation of a gas chromatograph-atmospheric pressure chemical ionization interface for an exactive orbitrap mass spectrometer. *J. Am. Soc. Mass Spectrom.* **2019**, *30*, 2369−2379.
(29) Mal, M.; Wong, S. A HILIC-Based UPLC-MS Method for the Separation of Lipid Classes from Plasma. *Waters Appl. Note* **2011**, No. 720004048en.
(30) Chambers, M. C.; Maclean, B.; Burke, R.; Amodei, D.; Ruderman, D. L.; Neumann, S.; Gatto, L.; Fischer, B.; Pratt, B.; Egertson, J.; et al.*et al.* A cross-platform toolkit for mass spectrometry and proteomics. *Nat. Biotechnol.* **2012**, *30*, 918−920.
(31) Clasquin, M. F.; Melamud, E.; Rabinowitz, J. D. LC-MS data processing with MAVEN: a metabolomic analysis and visualization engine. *Curr. Protoc. Bioinformatics* **2002**, *37*, 14.11. 1−14.11. 23.
(32) Wei, R.; Wang, J.; Su, M.; Jia, E.; Chen, S.; Chen, T.; Ni, Y. Missing value imputation approach for mass spectrometry-based metabolomics data. *Sci. Rep.* **2018**, *8*, No. 663.
(33) De Hoon, M. J.; Imoto, S.; Nolan, J.; Miyano, S. Open source clustering software. *Bioinformatics* **2004**, *20*, 1453−1454.
(34) Rühl, J.; Hein, E. M.; Hayen, H.; Schmid, A.; Blank, L. M. The glycerophospholipid inventory of *Pseudomonas putida* is conserved between strains and enables growth condition-related alterations. *Microbiol. Biotechnol.* **2012**, *5*, 45−58.
(35) Kondakova, T.; d'Heygère, F.; Feuilloley, M. J.; Orange, N.; Heipieper, H. J.; Poc, C. D. Glycerophospholipid synthesis and functions in *Pseudomonas*. *Chem. Phys. Lipids* **2015**, *190*, 27−42.
(36) Bhakoo, M.; Herbert, R. Fatty acid and phospholipid composition of five psychrotrophic *Pseudomonas* spp. grown at different temperatures. *Arch. Microbiol.* **1980**, *126*, 51−55.
(37) Curragh, H.; Flynn, O.; Larkin, M. J.; Stafford, T. M.; Hamilton, J. T.; Harper, D. B. Haloalkane degradation and assimilation by *Rhodococcus rhodochrous* NCIMB 13064. *Microbiology* **1994**, *140*, 1433−1442.
(38) Hamilton, J. T. G.; McRoberts, W. C.; Larkin, M. J.; Harper, D. B. Long-chain haloalkanes are incorporated into fatty acids by *Rhodococcus rhodochrous* NCIMB 13064. *Microbiology* **1995**, *141*, 2611−2617.
(39) Zhao, C.; Li, P.; Deng, Z.; Ou, H.-Y.; McGlinchey, R. P.; O'Hagan, D. Insights into fluorometabolite biosynthesis in *Streptomyces cattleya* DSM46488 through genome sequence and knockout mutants. *Bioorg. Chem.* **2012**, *44*, 1−7.
(40) Ma, L.; Bartholome, A.; Tong, M. H.; Qin, Z.; Yu, Y.; Shepherd, T.; Kyeremeh, K.; Deng, H.; O'Hagan, D. Identification of a fluorometabolite from *Streptomyces* sp. MA37:(2 R 3 S 4 S)-5-fluoro-2, 3, 4-trihydroxypentanoic acid. *Chem. Sci.* **2015**, *6*, 1414−1419.
(41) Dembitsky, V. M.; Srebnik, M. Natural halogenated fatty acids: their analogues and derivatives. *Prog. Lipid Res.* **2002**, *41*, 315−367.
(42) Murphy, C. D.; Schaffrath, C.; O'Hagan, D. Fluorinated natural products: the biosynthesis of fluoroacetate and 4-fluorothreonine in *Streptomyces cattleya*. *Chemosphere* **2003**, *52*, 455−461.
(43) Harper, D. B.; O'Hagan, D. The fluorinated natural products. *Nat. Prod. Rep.* **1994**, *11*, 123−133.
(44) O'Hagan, D. Understanding organofluorine chemistry. An introduction to the C−F bond. *Chem. Soc. Rev.* **2008**, *37*, 308−319.
(45) Agostini, F.; Sinn, L.; Petras, D.; Schipp, C. J.; Kubyshkin, V.; Berger, A. A.; Dorrestein, P. C.; Rappsilber, J.; Budisa, N.; Koksch, B. Multiomics analysis provides insight into the laboratory evolution of *Escherichia coli* toward the metabolic usage of fluorinated indoles. *ACS Cent. Sci.* **2021**, *7*, 81−92.
(46) Filimonova, V.; Goncalves, F.; Marques, J. C.; De Troch, M.; Goncalves, A. M. Fatty acid profiling as bioindicator of chemical stress in marine organisms: a review. *Ecol. Indic.* **2016**, *67*, 657−672.
(47) Barbier, O.; Arreola-Mendoza, L.; Del Razo, L. M. Molecular mechanisms of fluoride toxicity. *Chem. Biol. Interact.* **2010**, *188*, 319−333.
(48) Hirsh, D. J.; Lazaro, N.; Wright, L. R.; Boggs, J. M.; McIntosh, T. J.; Schaefer, J.; Blazyk, J. A new monofluorinated phosphatidylcholine forms interdigitated bilayers. *Biophys. J.* **1998**, *75*, 1858−1868.
(49) Gent, M. P.; Cottam, P. F.; Ho, C. Fluorine-19 nuclear magnetic resonance studies of *Escherichia coli* membranes. *Proc. Natl. Acad. Sci. U.S.A.* **1978**, *75*, 630−634.
(50) Gent, M.; Cottam, P.; Ho, C. A biophysical study of protein-lipid interactions in membranes of *Escherichia coli*. Fluoromyristic acid as a probe. *Biophys. J.* **1981**, *33*, 211−223.
(51) McDonough, B.; Macdonald, P. M.; Sykes, B. D.; McElhaney, R. N. Fluorine-19 nuclear magnetic resonance studies of lipid fatty acyl chain order and dynamics in *Acholeplasma laidlawii* B membranes. A physical, biochemical, and biological evaluation of monofluoropalmitic acids as membrane probes. *Biochemistry* **1983**, *22*, 5097−5103.
(52) McDonough, B.; Macdonald, P.; Sykes, B.; McElhaney, R. 19F-nuclear magnetic resonance study of glycerolipid fatty acyl chain order in *Acholeplasma laidlawii* B membranes. *Yale J. Biol. Med.* **1983**, *56*, 391.
(53) Wang, X.; Zheng, R.; Yao, Q.; Liang, Z.; Wu, M.; Wang, H. Effects of fluoride on the histology, lipid metabolism, and bile acid secretion in liver of *Bufo gargarizans larvae*. *Environ. Pollut.* **2019**, *254*, No. 113052.
(54) Gobelius, L.; Lewis, J.; Ahrens, L. Plant uptake of per-and polyfluoroalkyl substances at a contaminated fire training facility to evaluate the phytoremediation potential of various plant species. *Environ. Sci. Technol.* **2017**, *51*, 12602−12610.
(55) Loi, E. I. H.; Yeung, L. W.; Taniyasu, S.; Lam, P. K.; Kannan, K.; Yamashita, N. Trophic magnification of poly-and perfluorinated compounds in a subtropical food web. *Environ. Sci. Technol.* **2011**, *45*, 5506−5513.

https://doi.org/10.1021/acs.est.2c01454
Environ. Sci. Technol. 2022, 56, 8155−8166

(56) Sundström, M.; Ehresman, D. J.; Bignert, A.; Butenhoff, J. L.; Olsen, G. W.; Chang, S.-C.; Bergman, Å. A temporal trend study (1972−2008) of perfluorooctanesulfonate, perfluorohexanesulfonate, and perfluorooctanoate in pooled human milk samples from Stockholm, Sweden. *Environ. Int.* **2011**, *37*, 178−183.
(57) Wang, Q.; Ruan, Y.; Jin, L.; Zhang, X.; Li, J.; He, Y.; Wei, S.; Lam, J. C.; Lam, P. K. Target, nontarget, and suspect screening and temporal trends of per-and polyfluoroalkyl substances in marine mammals from the South China Sea. *Environ. Sci. Technol.* **2021**, *55*, 1045−1056.
(58) De Silva, A. O.; Armitage, J. M.; Bruton, T. A.; Dassuncao, C.; Heiger-Bernays, W.; Hu, X. C.; Kärrman, A.; Kelly, B.; Ng, C.; Robuck, A.; et al.*et al.* PFAS exposure pathways for humans and wildlife: a synthesis of current knowledge and key gaps in understanding. *Environ. Toxicol. Chem.* **2021**, *40*, 631−657.
(59) Dassuncao, C.; Pickard, H.; Pfohl, M.; Tokranov, A. K.; Li, M.; Mikkelsen, B.; Slitt, A.; Sunderland, E. M. Phospholipid levels predict the tissue distribution of poly- and perfluoroalkyl substances in a marine mammal. *Environ. Sci. Technol. Lett.* **2019**, *6*, 119−125.
(60) Fitzgerald, N. J. M.; Wargenau, A.; Sorenson, C.; Pedersen, J.; Tufenkji, N.; Novak, P. J.; Simcik, M. F. Partitioning and accumulation of perfluoroalkyl substances in model lipid bilayers and bacteria. *Environ. Sci. Technol.* **2018**, *52*, 10433−10440.
(61) Neidhardt, F. C. *Escherichia Coli and Salmonella: Cellular and Molecular Biology*, ASM Press: Washington, D.C., 1996; Vol. *1*.
(62) Torsvik, V.; Goksøyr, J.; Daae, F. L. High diversity in DNA of soil bacteria. *Appl. Environ. Microbiol.* **1990**, *56*, 782−787.
(63) Soltysiak, R.; Matsuura, F.; Bloomer, D.; Sweeley, C. D, L-α-Fluoropalmitic acid inhibits sphingosine base formation and accumulates in membrane lipids of cultured mammalian cells. *Biochim. Biophys. Acta, Mol. Cell Biol. Lipids* **1984**, *792*, 214−226.
(64) Yeung, L. W. Y.; Miyake, Y.; Taniyasu, S.; Wang, Y.; Yu, H.; So, M. K.; Jiang, G.; Wu, Y.; Li, J.; Giesy, J. P.; et al.*et al.* Perfluorinated compounds and total and extractable organic fluorine in human blood samples from China. *Environ. Sci. Technol.* **2008**, *42*, 8140−8145.
(65) Spaan, K. M.; van Noordenburg, C.; Plassmann, M. M.; Schultes, L.; Shaw, S.; Berger, M.; Heide-Jørgensen, M. P.; Rosing-Asvid, A.; Granquist, S. M.; Dietz, R.; et al.*et al.* Fluorine mass balance and suspect screening in marine mammals from the northern hemisphere. *Environ. Sci. Technol.* **2020**, *54*, 4046−4058.
(66) Yeung, L. W.; De Silva, A. O.; Loi, E. I.; Marvin, C. H.; Taniyasu, S.; Yamashita, N.; Mabury, S. A.; Muir, D. C.; Lam, P. K. Perfluoroalkyl substances and extractable organic fluorine in surface sediments and cores from Lake Ontario. *Environ. Int.* **2013**, *59*, 389−397.

https://doi.org/10.1021/acs.est.2c01454
Environ. Sci. Technol. 2022, 56, 8155−8166